

1 + 1 > 2: Detector-Empowered Video Large Language Model for Spatio-Temporal Grounding and Reasoning

Shida Gao^{1*} Feng Xue^{2*} Xiangfeng Wang^{1*} Anlong Ming^{1†} Teng Long² Yihua Shao³
 Haozhe Wang⁴ Zhaowen Lin¹ Wei Wang⁵ Nicu Sebe²

¹Beijing University of Posts and Telecommunications ²University of Trento

³Institute of Automation, Chinese Academy of Sciences

⁴Hong Kong University of Science and Technology ⁵ZTE Corporation

Abstract

*Spatio-temporal grounding and reasoning aims to locate the temporal segment and spatial region of an event in a video given a user query, while also reasoning about semantics such as causality, temporal order, and action relationships. To achieve this, current MLLMs primarily treats bounding boxes as text tokens and generates them autoregressively. However, such autoregressive spatial decoding leads to very-long output sequences, causing spatial errors to accumulate over time and the localization results to progressively drift across a video. To address this, we present a Detector-Empowered Video LLM, short for **DEViL**, which couples a Video LLM with an open-vocabulary detector (OVD). Specifically, the MLLM and detector are connected via a reference-semantic token (RST) that distills the user query into a rich semantic representation. Unlike tokens that merely serve as spatial prompts or segmentor switches, the RST functions as both a control signal and a replacement for the OVD’s text embedding, enabling end-to-end learning of both referential understanding and spatial localization. Furthermore, we propose a tube-mined temporal regularization (TTReg) within OVD, which drives the OVD to generate temporally-consistent queries for target objects, thereby ensuring effective temporal association. Experiments demonstrate that **DEViL** achieves strong performance across various fine-grained video understanding tasks, particularly STVG and GroundedVQA. Code will be released on <https://github.com/gaostar123/DeViL>.*

1. Introduction

Driven by the recent progress of multimodal large language models (MLLMs), video understanding has rapidly progressed from **coarse-grained** reasoning tasks, such as video question answering (VQA) [2, 16], captioning (VC)

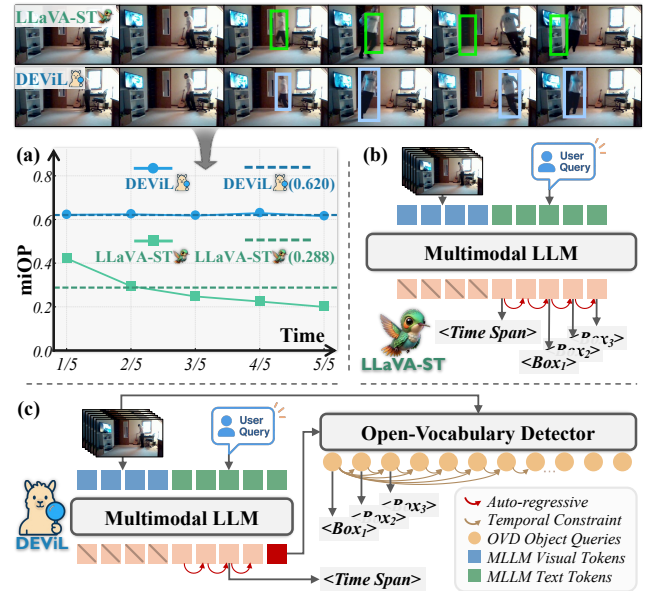


Figure 1. **Comparing LLaVA-ST [36] and DEViL.** (a) The mean IoU between predicted and ground-truth boxes (miOP) across the ground-truth interval. (b) Structure of LLaVA-ST. (c) Structure of our method, **DEViL**. For each video on VidSTG [79], we evenly split the ground-truth segment into 5 parts and compute miOP on each part, producing 5 points along the x-axis (1/5 to 5/5). Long-sequence suffer from error accumulation and localization drift.

[6, 65], and summarization (VS) [23, 58], toward **fine-grained** spatio-temporal reasoning, including video kinematics [71] and grounded VQA (GVQA) [32, 64]. With this shift, spatio-temporal video grounding (STVG) serves as a natural bridge between coarse video understanding and fine-grained spatio-temporal reasoning. STVG requires locating both the temporal segment and the spatial trajectory (frame-wise bounding boxes) of the object mentioned in the user query. Recent studies have endowed MLLMs with spatio-temporal localization and reasoning, yielding remarkable results on STVG and related tasks. A prominent line of

*Equal contributions

†Corresponding author

work, *e.g.*, LLaVA-ST [36], textualizes frame-wise bounding boxes and time spans, and then auto-regressively decodes these tokens with a language head, unifying grounding and reasoning under a single generative pipeline. However, treating coordinates as text brings two main problems. First, the model receives no IoU-based or cross-frame consistency feedback and thus cannot directly judge geometric accuracy or temporal smoothness. Second, this text-based decoding produces very long output sequences, aggravating exposure bias: early errors in predicted coordinates are fed back into later steps, leading to accumulated errors and localization drift over time. Fig. 1 illustrates this intuitively. LLaVA-ST’s mean Intersection-over-Prediction (miOP) gradually decreases over videos consistently. Visually, the predicted boxes increasingly deviates from the true object and tends to degenerate into a fixed regions in later frames. This motivates us to rethink how spatio-temporal grounding should be performed in MLLMs beyond purely text decoding.

To address the issues above, we propose a Detector-Empowered Video LLM, short for DEViL, which couples an MLLM with an open-vocabulary detector (OVD), while keeping the ability to unify spatio-temporal video grounding and reasoning within a single model. Specifically, we first distill the user query into a high-level OVD-compatible semantic token produced by the MLLM, called Reference-Semantic Token (RST). Neither a spatial prompt nor simple module-switching tag, RST is a pure and rich semantic token to occupies the OVD’s text-embedding input, letting the MLLM and detector jointly learn to express and localize complex language descriptions. Then, to improve cross-frame box consistency, we propose Tube-mined Temporal Regularization (TTReg). TTReg exploits cross-frame correlations to fine-tune the OVD in an end-to-end manner, encouraging temporally consistent detection. With only minor changes to the original OVD, TTReg produces tracking-like results. Extensive experiments demonstrate DEViL outperforms other MLLM tailored for STVG with capabilities on spatio-temporal video reasoning tasks, *e.g.*, GVQA. In summary, the major contributions of our work are:

- In the field of spatio-temporal grounding of MLLM, we reveals the exposure bias and sequence error accumulation caused by autoregressive latent space and textualized coordinate decoding.
- We propose DEViL to perform both spatio-temporal video grounding and reasoning. By connecting OVDs and MLLMs in the language space via a proposed RST, it avoiding the sequence error accumulation while providing a scalable spatial grounding module.
- We design a tube-mined temporal regularization, making minimal intrusive modifications to OVD and transforming it into a trainable tracker. This enables DEViL to achieve more stable spatio-temporal results.

2. Related Works

2.1. Multimodal LLMs for Video Understanding

Current MLLMs mainly target video understanding at a coarse level—Video Question Answering (VQA) [17, 37, 48, 57, 77] and are being extended toward fine-grained dimensions, including Temporal Video Grounding (TVG) [1, 21, 22, 25, 26], Referring Video Object Segmentation (RVOS) [4, 41, 66, 73], and Grounded VQA (GVQA) [18, 51, 61]. A few models further attempt Spatio-Temporal Video Grounding (STVG) within the MLLM framework [36, 50, 62]; however, textualized coordinate decoding introduces exposure bias and typically lacks explicit cross-frame constraints, degrading long-horizon performance and temporal coherence. To address these issues, DEViL replaces the detector’s text-embedding space with a learned Reference–Semantic Token (RST) and jointly localizes when and where in a single pass, yielding temporally consistent tubes while preserving broad video reasoning ability—enabling one model to handle VQA, TVG, GVQA, and STVG in a synergistic manner.

2.2. Spatial-Temporal Grounding and Reasoning

Recent MLLM-based approaches to video evidence localization can be roughly grouped into three types. First, *video spatial grounding* models predict frame-wise masks or boxes under language guidance while treating time implicitly through tracking [4, 41, 66, 73], so they usually do not output explicit start-end timestamps or complete what–when–where chains. Second, *video temporal grounding* methods align queries with temporal segments [22, 25, 51, 55, 61, 63], but spatial localization is coarse and not modeled as frame-wise tubes. Third, *spatio-temporal video grounding* within MLLMs predicts both when and where by textualizing boxes and spans for autoregressive decoding or by regressing coordinates from hidden states [36, 50, 62]. However, these designs keep spatial representation on the language side, where coordinates lack explicit IoU-based feedback, cross-frame association is weak, and long decoding sequences suffer from exposure bias and drifting boxes. DEViL also targets spatio-temporal grounding and reasoning, but instead couples an MLLM with an open-vocabulary detector via a learned Reference–Semantic Token (RST) that replaces the detector’s text-embedding input, and applies tube-mined temporal regularization (TTReg) to stabilize query features and boxes across frames. This preserves the instruction-following and general reasoning ability of the MLLM while leveraging detector-level spatial accuracy and temporally consistent tubes, enabling a single model to handle STVG, TVG, and GVQA in a unified manner.

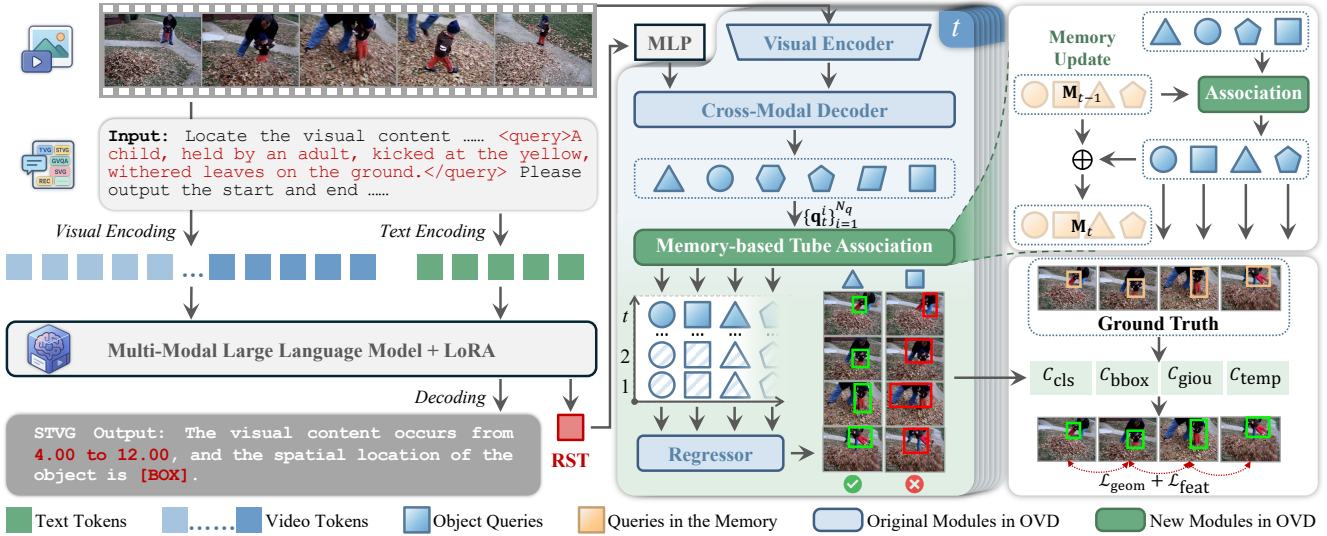


Figure 2. Overall architecture of DEVIL. Given a video and query, the MLLM encodes them and emits a special [BOX] token whose hidden state serves as the Reference-Semantic Token (RST). RST replaces the text embedding of the open-vocabulary detector (OVD) to drive object queries. A memory-based tube association maintains query identity across frames, while tube-mined temporal regularization (TTReg) regularizes ground-truth-aligned tubes to learn temporally consistent boxes. Note that the classification head of OVD is omitted for the purpose of simplifying expression and visualization.

3. Method

3.1. Network Architecture of DEVIL

The overall architecture of DEVIL is shown in Fig. 2. It consists of two components: a multimodal large language model (MLLM) and an open-vocabulary detector (OVD), connected through a specialized embedding called Reference-Semantic Token (RST). RST not only serves as the trigger for invoking the OVD, but also injects rich semantic context from the MLLM, guiding the detector toward accurate and temporally consistent localization.

Multimodal Large Language Model. We employ a pre-trained MLLM for video understanding and aggregating contextual information. Specifically, given a video $\{v_t\}_{t=1}^T$ with T frames and a textual query Q as inputs, a vision encoder and a text encoder first process the inputs v_t to produce frame-level visual embeddings and token-level text embeddings. These embeddings are then fed into a MLLM, which outputs a sequence of hidden states $\mathbf{H}_{\text{llm}} \in \mathbb{R}^{L \times D_{\text{llm}}}$, where L is the output token number and D_{llm} is the hidden dimension. Our proposed RST is included in \mathbf{H}_{llm} , while the remaining hidden states are decoded into text outputs.

Open-Vocabulary Detector. We use an query-based OVD as an external spatial executor of the MLLM. This choice is motivated by two observations: (1) Both OVDs and MLLMs operate in language spaces, providing a target space for learning our RST. (2) Detectors trained on standard detection corpus already provide reliable localization. Even an OVD fine-tuned on COCO only is effective

enough for MLLM. In DEVIL, we modify OVD minimal-intrusively to a tracker to facilitates cross-frame consistency mined by object tubes, illustrated in Sec. 3.2.

Reference-Semantic Token. In DEVIL, the RST serves as the bridge between the MLLM and the OVD. Specifically, we first add a special token, denoted as [BOX], to the MLLM’s vocabulary to indicate that spatial grounding is required. If so, the MLLM outputs a textual result containing [BOX]. Correspondingly, the hidden state of [BOX] can be denoted as $\mathbf{z}_{\text{rst}} \in \mathbb{R}^{D_{\text{llm}}}$. Then, to inject RST into the OVD as a language query, we map \mathbf{z}_{rst} to the detector’s text-embedding space with a learnable linear projection:

$$\mathbf{e}_{\text{text}} = \mathbf{W} \mathbf{z}_{\text{rst}} + \mathbf{b}, \quad \mathbf{e}_{\text{text}} \in \mathbb{R}^{D_{\text{det}}} \quad (1)$$

where $\mathbf{W} \in \mathbb{R}^{D_{\text{det}} \times D_{\text{llm}}}$ and $\mathbf{b} \in \mathbb{R}^{D_{\text{det}}}$ are learnable parameters. Finally, we replace the OVD’s original text embedding with \mathbf{e}_{text} and feed it to the OVD’s language branch as the cross-attention query. The OVD aligns \mathbf{e}_{text} with per-frame visual features and outputs frame-wise bounding box predictions. The entire pipeline is trained in an end-to-end manner to teach the MLLM to generate context-aware RSTs that guide precise localization, which is described in detail in Sec. 3.3.

3.2. Tube-Mined Temporal Regularization

To achieve consistent localization across consecutive frames in the OVD, a straightforward approach is to apply the Hungarian algorithm for cross-frame tube association [39]. However, object appearance may varies widely across

Question: The small guinea pig is eating grass.

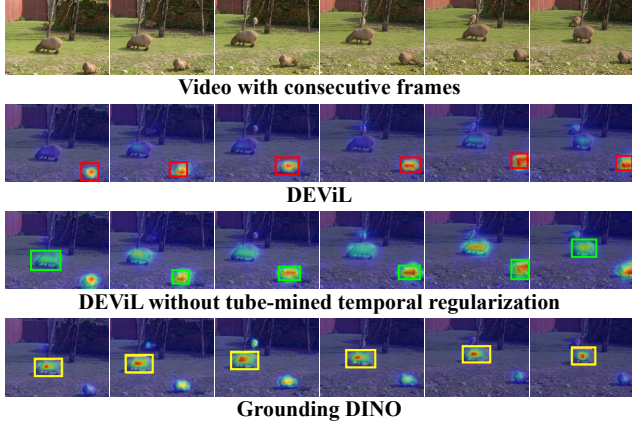


Figure 3. **Attention and detection comparison** between the [BOX]-induced RST/text feature and image features (red: w/ TTRReg; green: w/o). TTRReg keeps attention and boxes on the target, while removing it causes scattered attention and jitter. Grounding DINO (yellow boxes) instead uses text-image attention that focuses on a distractor.

frames, causing the OVD’s per-frame object queries to drift and leading to unreliable associations. To address this, we propose tube-mined temporal regularization (TTRReg), transforming the OVD into a tracker with minimal modification. In the following, we first describe the tube association and analyze its failure modes that motivate TTRReg.

Memory-based Tube Association. Given the video $\{v_t\}_{t=1}^T$ with T frames and the RST-induced text token e_{text} , the OVD in DEViL follows the original detection manner to compute a set of object queries in each frame:

$$\{\mathbf{q}_t^i\}_{i=1}^N = \text{Dec}(\{\mathbf{q}\}^0; f(v_t), e_{\text{text}}) \quad (2)$$

where $f(\cdot)$ denotes the OVD’s visual encoder, $\{\mathbf{q}\}^0$ is a initial query set, and $\text{Dec}(\cdot)$ is the OVD’s decoding process. Next, we select top- N_q queries from $\{\mathbf{q}_t^i\}_{i=1}^N$, denoted as $\{\mathbf{q}_t^i\}_{i=1}^{N_q}$, for memory-based tube association, as shown in Fig. 2. Following [39], for the first frame $t = 1$, we establish a reference memory $\mathbf{M}_1 = \{\hat{\mathbf{q}}_1^i\}_{i=1}^{N_q}$, where $\hat{\mathbf{q}}_1^i = \mathbf{q}_1^i$. Then, for the subsequent frame $t > 1$, their queries $\{\mathbf{q}_t^i\}_{i=1}^{N_q}$ are matched against the memory from the previous frame \mathbf{M}_{t-1} using the Hungarian algorithm based on cosine similarity. In this process, the queries $\{\mathbf{q}_t^i\}_{i=1}^{N_q}$ are re-ordered to align with $\mathbf{M}_{t-1} = \{\hat{\mathbf{q}}_{t-1}^i\}_{i=1}^{N_q}$, then update the memory with an exponential moving average:

$$\mathbf{M}_t = (1 - \alpha_t) \mathbf{M}_{t-1} + \alpha_t \text{reorder}(\{\mathbf{q}_t^i\}_{i=1}^{N_q}), \quad (3)$$

where α_t is an adaptive update rate. This design tries to ensure that a single query slot consistently tracks the same object instance throughout the video clip.

Despite this intent, tube association is not always reliable because object features in video vary. As illustrated in Fig. 3, the attention inside the object region fluctuates across frames, yielding unstable similarity between the corresponding per-frame queries. The proposed TTRReg aims to alleviate this. It first mines an object tube that exhibits the highest alignment with the ground truth, and then achieves a cross-frame regularization on that tube to align the per-frame object queries, improving association robustness.

Ground-Truth-Aligned Tube Mining. To encourage temporally smooth detection, we select the object tube, *i.e.*, $\{\mathbf{q}_t^i\}_{t=1}^T$, that is most similar to the ground truth from all object tubes $\{\{\mathbf{q}_t^i\}_{t=1}^T | i \in [1, N_q]\}$, facilitating cross-frame constraint supervision. Following Grounding-DINO [43], we employ its three cost functions:

- C_{cls} penalizes semantic mismatch between the query and the ground-truth phrase.
- C_{bbox} penalizes coordinate error and encourage boxes closer to the ground truth.
- C_{giou} penalizes overlap/shape error and favors boxes with good coverage.

To penalizes cross-frame spatial jitter, we employ a temporal consistency cost that is defined as the average “1 - GIoU” over all adjacent frame pairs:

$$C_{\text{temp}}^i = \frac{1}{T-1} \sum_{t=1}^{T-1} (1 - \text{GIoU}(b_t^i, b_{t+1}^i)), \quad (4)$$

where b_t^i is the predicted bounding box for \mathbf{q}_t^i . The final cost for matching is a weighted sum: $C = \lambda_{\text{cls}} C_{\text{cls}} + \lambda_{\text{bbox}} C_{\text{bbox}} + \lambda_{\text{giou}} C_{\text{giou}} + \lambda_{\text{temp}} C_{\text{temp}}$. This encourage the model to select predicted tubes that exhibit high spatial coherence. In this way, the selected tube can be formulated as $\{(b_t^*, \mathbf{q}_t^*)\}_{t=1}^T$, *i.e.*, per-frame boxes with their queries.

Cross-Frame Temporal Regularization. After assigning the ground-truth label to the best-matched predicted tube, we apply an explicit temporal consistency loss to supervise its change over time. This loss consists of two components: a feature consistency loss ($\mathcal{L}_{\text{feat}}$) and a geometric consistency loss ($\mathcal{L}_{\text{geom}}$). They are defined as:

$$\begin{aligned} \mathcal{L}_{\text{feat}} &= \frac{1}{T-1} \sum_{t=1}^{T-1} \left(1 - \frac{\mathbf{q}_t^* \cdot \mathbf{q}_{t+1}^*}{\|\mathbf{q}_t^*\| \|\mathbf{q}_{t+1}^*\|} \right), \\ \mathcal{L}_{\text{geom}} &= \frac{1}{T-1} \sum_{t=1}^{T-1} (1 - \text{GIoU}(b_t^*, b_{t+1}^*)). \end{aligned} \quad (5)$$

These losses explicitly enforce that the visual features and spatial coordinates of the queried object remain over short time intervals, thereby fine-tuning each module of the OVD to output temporally-consistent queries and bounding boxes, making the OVD works like a tracker.

3.3. Training Paradigm and Inference

In training, we adapt the MLLM only through LoRA [24], so that it preserves its pretrained video understanding while

Model	What	Chain1 (When)		Chain1 (Where)		Chain2 (Where)		Chain2 (When)		Overall	
	Acc	R1@0.5	m.tIoU	AP@0.5	m.vIoU	AP@0.5	m.vIoU	R1@0.5	m.tIoU	mAM	mLGM
GPT-4o [27]	60.8	10.4	16.7	2.8	6.5	1.2	3.0	10.0	12.8	26.8	38.2
Gemini-2-Flash [12]	53.0	15.9	24.5	0.9	4.6	0.6	2.2	15.2	23.8	26.9	35.6
Video-LLaMA3 [75]	41.9	19.8	23.0	0.1	0.9	0.0	0.2	20.4	23.1	21.7	27.0
LLaVA-Video [78]	49.5	6.3	10.5	0.2	1.9	0.3	1.3	5.5	12.2	20.8	27.3
VideoChat2 [38]	36.2	13.1	13.7	0.1	2.5	0.3	1.0	12.1	12.5	17.0	20.3
Oryx-1.5-7B [46]	20.5	4.5	13.5	2.2	10.1	1.0	3.5	5.6	14.8	15.1	13.8
InternVL-2.5-8B [9]	44.2	4.9	8.7	0.0	0.7	0.0	0.1	3.8	7.8	17.6	24.9
Qwen2.5-VL-7B [3]	54.5	8.9	11.5	8.4	13.6	1.4	2.0	5.4	7.6	24.0	32.4
TimeChat-7B [55]	26.4	8.7	12.01	—	—	—	—	8.5	13.6	13.1	14.8
VTimeLLM-7B [25]	41.5	10.9	17.1	0.0	0.21	0.0	0.0	2.1	5.96	17.7	22.0
TRACE [21]	17.6	14.1	19.1	—	—	—	—	12.0	17.1	12.0	13.3
Sa2VA-8B [73]	16.4	0.0	0.1	34.18	32.3	40.4	37.5	0.0	0.0	17.1	20.3
LLaVA-ST [35]	55.0	17.4	19.9	20.1	22.2	8.2	9.5	15.7	23.4	30.8	40.6
DEViL (Ours)	34.3	19.7	27.5	40.3	37.2	44.5	41.7	16.7	25.0	33.2	40.7

Table 1. Results on the V-STaR [11] benchmark under the two Reverse Spatio-Temporal Reasoning chains. *What* reports VQA accuracy (Acc). For each chain, *When* evaluates temporal grounding with R1@0.5 and mean temporal IoU (m.tIoU), while *Where* evaluates spatial grounding with AP@0.5 and mean visual IoU (m.vIoU). mAM and mLGM are the arithmetic and logarithmic geometric means over {Acc, m.tIoU, m.vIoU} across both chains. Bold numbers denote the best performance.

learning to emit effective RSTs. In parallel, we fine-tune the OVD for visual grounding and higher temporal consistency using TTReg. To achieve the goals above, our training follows a three-stage curriculum, with each stage corresponding to specific modules, as described below.

Stage 1: Bridging MLLM and OVD. The preliminary training stage focuses on establishing the fundamental connection between the MLLM and the detector. Using image-based referring expression datasets (*RefCOCO* [30], *RefCOCO+* [30], *RefCOCOg* [49]), DEViL learns to adaptively output a task-specific [BOX] token that encapsulates referential spatial semantics according to the input text.

Stage 2: Temporal Alignment for MLLM. In this stage, we enhance the temporal alignment capability of the MLLM. We freeze the OVD and fine-tune only the MLLM on temporal grounding datasets (*TACoS* [54], *ActivityNet Captions* [31], *QVHighlights* [33]). Instead of predicting bounding boxes, the MLLM is required to determine when the referenced event occurs.

Stage 3: Spatio-Temporal Collaboration Training. In the final stage, we unfreeze the whole architecture and jointly optimize the MLLM and the detector on a unified spatio-temporal corpus constructed from public datasets via data reformulation and pseudo-labeling. Following LLaVA-ST [36], we enhance and revise the textual queries in training data of *HC-STVG v1/v2* [60] and *VidSTG* [79] into instruction-style inputs suitable for MLLM training, while preserving their human-labeled spatio-temporal tubes.

To enrich spatial supervision, we re-purpose the static

grounding set SA-V [53] by assigning time spans to obtain tube-level labels. In addition, we implement an automatic pipeline that combines a strong detector (MM-Grounding-DINO [80]), a powerful REC VLM (VLM-R1 [56]) and a tracker (SUTrack [8]) to generate dense object tubes, which is then used to lift the Stage-2 temporal grounding datasets (*TACoS*, *ActivityNet Captions*, *QVHighlights*) to the spatio-temporal setting. The final corpus contains 196k spatio-temporally annotated samples, combining human-labeled and automatically generated tubes. During this stage, we apply Tube-mined Temporal Regularization (TTReg) to enforce cross-frame alignment within tube-level queries: the MLLM produces RSTs and the detector executes them, forming a collaborative closed loop between high-level reasoning and low-level grounding. To foster reproducibility, we will release reformatted annotations, automatic-labeling method and pseudo labels.

Unified Inference for Multiple Tasks. At inference, DEViL runs in an *intent-conditioned* manner: the MLLM either returns text-only outputs or emits the special [BOX] token and its RST to trigger the OVD for grounding. For grounding-required cases, the OVD together with the memory-based tube association in Eq. (3) produces N_q tube hypotheses $\{\tau_i\}_{i=1}^{N_q}$, where $\tau_i = \{(s_t^i, b_t^i)\}_{t=1}^T$ denotes the confidence s_t^i given by the classification head of OVD and box b_t^i of the i -th query at frame t . The final tube index \hat{i} is selected by average confidence:

$$\hat{i} = \arg \max_{i \in [1, N_q]} \frac{1}{T} \sum_{t=1}^T s_t^i. \quad (6)$$

Model	Setting	HC-STVG v1				HC-STVG v2			
		m_tIoU	m_vIoU	vIoU@0.3	vIoU@0.5	m_tIoU	m_vIoU	vIoU@0.3	vIoU@0.5
STVGBert [59]	Fully Sup	-	20.4	29.4	11.3	-	-	-	-
TubeDETR [68]		43.7	32.4	49.8	23.5	53.9	36.4	58.8	30.6
STCAT [28]		49.4	35.1	57.7	30.1	-	-	-	-
STVGFormer [42]		-	36.9	62.2	34.8	58.1	38.7	65.5	33.8
CG-STVG [19]		52.8	38.4	61.5	36.3	60.0	39.5	64.5	36.3
TA-STVG [20]		53.0	39.1	63.1	36.8	60.4	40.2	65.8	36.7
LLaVA-ST* [36]	LLM	22.2	9.4	8.1	2.8	21.6	8.7	6.0	1.2
DEViL (Ours)		54.7	36.2	59.9	31.8	58.0	36.5	58.0	31.8

Model	Setting	VidSTG (Declarative Sentence)				VidSTG (Interrogative Sentence)			
		m_tIoU	m_vIoU	vIoU@0.3	vIoU@0.5	m_tIoU	m_vIoU	vIoU@0.3	vIoU@0.5
STGVF [60]	Fully Sup	-	21.6	29.8	18.9	-	-	-	-
STVGBert [59]		-	24.0	30.9	18.4	-	22.5	26.0	16.0
TubeDETR [68]		48.1	30.4	42.5	28.2	46.9	25.7	35.7	23.2
STCAT [28]		50.8	33.1	46.2	32.6	49.7	28.2	39.2	26.6
STVGFormer [42]		-	33.7	47.2	32.8	-	28.5	39.9	26.2
CG-STVG [19]		51.4	34.0	47.7	33.1	49.9	29.0	40.5	27.5
TA-STVG [20]		51.7	34.4	48.2	33.5	50.2	29.5	41.5	28.0
LLaVA-ST [36]	LLM	28.7	8.2	10.6	5.0	27.5	6.8	8.3	3.9
DEViL (Ours)		49.0	32.0	43.7	30.7	47.3	27.7	37.5	25.5

Table 2. Comparison on three STVG benchmarks: HC-STVG v1/v2 [60], and VidSTG [79] (declarative and interrogative queries). Metrics include m_tIoU (mean temporal IoU), m_vIoU (mean spatio-temporal IoU), and vIoU@ τ (fraction of samples with vIoU $\geq \tau$). Bold numbers denote the best performance. * indicates the zero-shot setting.

We then output the trajectory $\{\hat{b}_t^i\}_{t=1}^T$ as the evidence for spatio-temporal grounding and reasoning.

4. Experiments

In this section, we first elaborate on the implementation details (Sec. 4.1) of DEViL. Next, we conduct extensive testing (Sec. 4.2) under *spatio-temporal video grounding*, *temporal video grounding*, *grounded video question and answering*, and *common video understanding* to verify its effectiveness and generalization. Finally, we validate the effectiveness of each module by ablation studies (Sec. 4.3).

4.1. Implements Details

We initialize the vision encoder with SigLIP [74] and the LLM with Qwen2.5-7B [70]; checkpoints are loaded from the public VideoLLaMA3-7B [75] release. The projector is a two-layer MLP with GELU. The OVD is Grounding DINO [43] with a Swin-B [45] backbone pre-trained on COCO only. Across Stage-1/2/3 we freeze the MLLM vision encoder and fine-tune the LLM with LoRA [24] ($\alpha = 16$, $r = 64$). In Stage-2 the detector is frozen, while in Stages-1 and -3 it is tunable. We use AdamW for optimization. The detector uses a learning rate of 1×10^{-4} in all trainable stages, while the LLM and the projector use 1×10^{-5} , and the global batch sizes for Stage-1/2/3 are 128/32/8, respectively. Clips are uniformly sampled to

$T = 64$ frames per video. For memory-based tube association, we keep the top $N_q = 15$ queries per frame to form tube hypotheses and set the EMA update rate to $\alpha_t = 0.1$. In the Hungarian matcher and TTReg, following DETR [5], the cost weights are set to $\lambda_{cls} = 1$, $\lambda_{bbox} = 5$, $\lambda_{giou} = 3$, $\lambda_{temp} = 2$ and $\lambda_{feat} = 1$, which are then used in training. All experiments are conducted on four A800 GPUs, and training a single epoch over all datasets takes about six days.

4.2. Main Comparisons

Spatio-Temporal Video Grounding and Reasoning. We first evaluate DEViL on four STVG benchmarks: the unified V-STaR benchmark [11], HC-STVG v1 and v2 [60], VidSTG with declarative and interrogative queries [79].

On V-STaR [11], stronger temporal and spatial grounding translates into the best scores among all compared models. Our method achieves the best temporal and spatial localization on both Chain1 and Chain2. In particular, its m_vIoU exceeds that of the runner-up Sa2VA by 4.9% on Chain1 and 4.2% on Chain2. DEViL attains lower VQA accuracy, *i.e.*, ACC, than several VideoQA-oriented MLLMs, which we attribute to using only grounding-style supervision without any additional VQA instruction data. In contrast, it achieves substantially stronger spatio-temporal grounding and reasoning, leading to the best overall scores among all methods, with mAM of 33.2 and mLGM of 40.7

Model	Acc@GQA	mIoP	IoP@0.5	mIoU	IoU@0.5
VIOLETv2 [14]	12.8	23.6	23.3	3.1	1.3
SeViLA [72]	16.6	29.5	22.9	21.7	13.8
LangRepo [29]	17.1	31.3	28.7	18.5	12.2
FrozenBiLM NG+ [69]	17.5	24.2	23.7	9.6	6.1
VideoStreaming [52]	17.8	32.2	31.0	19.3	13.3
LLoVi [76]	24.3	37.3	36.9	20.0	15.3
Grounded-VideoLLM [61]	26.7	34.5	34.4	21.1	18.0
HawkEye [63]	—	—	—	25.7	19.5
VideoChat-TPO [67]	25.5	35.6	32.8	27.7	23.4
DEViL (Ours)	36.3	48.1	48.1	27.9	23.4

Table 3. Results on the NExT-GQA [64] grounded VideoQA benchmark. Acc@GQA measures grounded QA accuracy, while mIoP/IoP@0.5 and mIoU/IoU@0.5 evaluate temporal localization and spatial overlap between predicted and ground-truth evidence segments. Bold numbers denote the best performance.

Model	Charades-STA			
	R1@0.3	R1@0.5	R1@0.7	m.tIoU
Video-LLaMA[77]	25.2	10.6	3.4	16.8
SeViLA[72]	27.0	15.0	5.8	18.3
Video-ChatGPT[48]	27.2	6.2	1.9	19.7
Valley[47]	28.4	1.8	0.3	21.4
VideoChat[37]	32.8	8.6	0.0	25.9
Momenter[51]	42.6	26.6	11.6	28.5
VTimeLLM[25]	51.0	27.5	11.4	31.2
TimeChat[55]	—	32.2	13.4	—
VTG-LLM[22]	—	33.8	15.7	—
HawkEye[63]	50.6	31.4	14.5	33.7
Grounded-VideoLLM[61]	54.2	36.4	19.7	36.8
LLaVA-ST[36]	63.1	44.8	23.4	42.4
DEViL (Ours)	72.6	51.5	25.2	47.7

Table 4. Performance on the Charades-STA [15] temporal grounding benchmark. We report R1@0.3/0.5/0.7 and mean temporal IoU (m.tIoU). Bold numbers denote the best performance.

even though these metrics are biased toward question answering. In principle, DEViL can be combined with standard VQA fine-tuning to further boost pure QA scores, but we intentionally keep the training protocol minimal in this work so that the gains in AM/LGM can be clearly attributed to detector-empowered structure. On HC-STVG *v1/v2*, DEViL essentially achieved the performance level of a fully supervised algorithms. On VidSTG, DEViL remains robust under different query styles, reaching 32.0 mean spatio-temporal IoU on declarative queries and 27.7 on interrogative queries, compared with 8.2 and 6.8 for LLaVA-ST [35], while staying competitive with fully supervised systems [19, 20, 28, 42, 60, 68].

Temporal Video Grounding (TVG). As shown in Table 4, we evaluate DEViL on the Charades-STA benchmark, DEViL achieves 51.5 R1@0.5 and 47.7 mean temporal IoU, surpassing Grounded-VideoLLM [61] and improving over LLaVA-ST [36] by 6.7 R1@0.5 and 5.3 mean tem-

Model	MVBench	TempCompass	VideoMME (w/o / w/ subs)
TimeChat-7B [55]	38.5	38.9	34.7 / —
VideoLLaMA2-7B [10]	54.6	43.4	47.9 / —
VideoChat2-7B [38]	51.1	48.81	42.3 / 54.6
Video-LLaVA-7B [40]	43.0	49.77	39.9 / 41.6
LLaVA-NeXT-Video-7B [34]	53.1	53.75	33.7 / —
TimeMarker [7]	67.4	60.4	57.3 / —
LLaVA-ST [35]	64.2	—	— / —
DEViL (Ours)	65.4	63.75	57.7 / 62.4

Table 5. Comparison on MVBench [38], TempCompass [44], and VideoMME [13] (without/with subtitles); all numbers are average accuracy scores. Bold numbers denote the best performance.

poral IoU. These results show that DEViL provides strong temporal localization ability among current video MLLMs.

Grounding Video QA (GQA). As shown in Table 3, we evaluate **DEViL** on the NExT-GQA benchmark, which jointly measures answering accuracy and evidence grounding. DEViL achieves 36.3 Acc@GQA, 48.1 mIoP and 27.9 mIoU, clearly surpassing recent video grounding QA models such as LLoVi [76], Grounded-VideoLLM [61], Hawk-Eye [63] and VideoChat-TPO [67].

Video Understanding. As shown in Table 5, we further assess **DEViL** on generic video understanding benchmarks, including MVBench [38], TempCompass [44], and VideoMME [13]. DEViL attains 65.4 on MVBench, close to the best score of TimeMarker [7], and achieves the highest accuracy on TempCompass with 63.75. On VideoMME, it also sets new highs with 57.7 without subtitles and 62.4 with subtitles, outperforming prior video LLMs such as TimeChat [55], VideoLLaMA2 [10], VideoChat2 [38], Video-LLaVA [40], LLaVA-NeXT-Video [34], and LLaVA-ST [35], indicating strong general video reasoning ability.

Qualitative analysis. Fig. 4 compares DEViL and LLaVA-ST on two cases: the first requires localizing the cart pushed by the child, and the second requires localizing the horse on the right side of the video. Both models can answer the textual query correctly, but LLaVA-ST’s autoregressive box decoding leads to temporal over- and under-coverage as well as box drift, whereas DEViL produces shorter event durations and more stable object trajectories.

4.3. Ablation Study

We next dissect how the temporal enhancer in DEViL contributes to the STVG gains. We focus on the tube-mined temporal regularization (TTReg) in Sec. 3.2, decomposed into **Ground-Truth-Aligned Tube Mining (GTM)** and **Cross-Frame (Temporal) Regularization (CFR)**, and on the test-time **Memory-based Tube Association (MTA)** in Eq. (3). Unless otherwise stated, we follow the settings in Sec. 4 and report m.tIoU and m.vIoU on HC-STVG *v1/v2*.

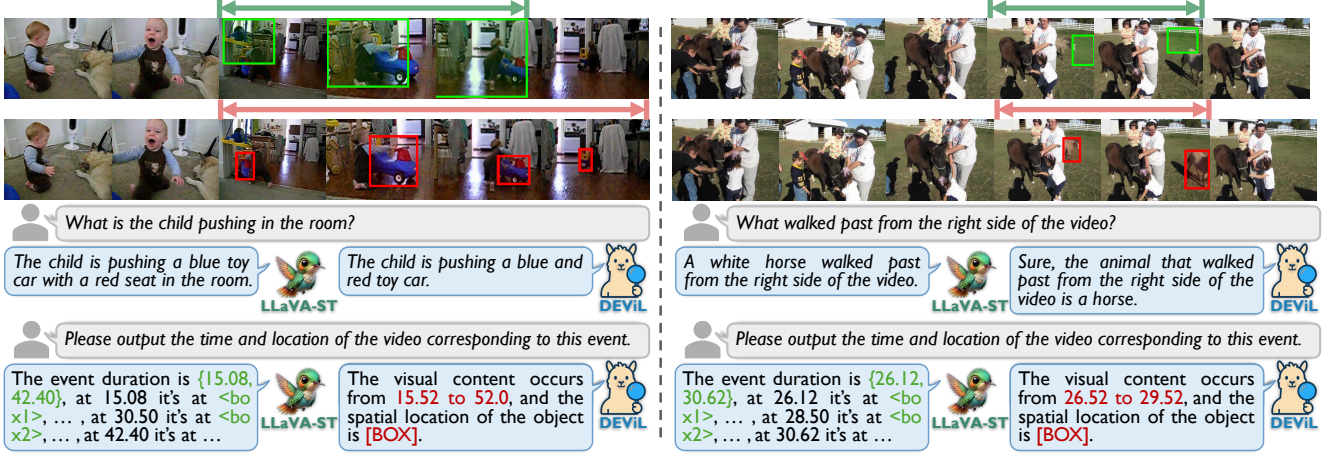


Figure 4. **Qualitative comparison between LLaVA-ST and DEViL.** For each example, the first row **green** shows LLaVA-ST’s predictions, while the second row **red** shows those of **DEViL**.

TTReg Modules		HC-STVG v1		HC-STVG v2	
GTM	CFR	m_tIoU	m_vIoU	m_tIoU	m_vIoU
✗	✗	53.3	35.5	57.4	35.8
✓	✗	54.4	35.8	57.6	36.1
✗	✓	54.9	35.6	57.9	35.5
✓	✓	54.7	36.2	58.0	36.5

Table 6. Training-time tube-mined temporal regularization (TTReg) on HC-STVG v1/v2. We toggle Ground-Truth-Aligned Tube Mining (GTM) and Cross-Frame (Temporal) Regularization (CFR) in Sec. 3.2. ✓ indicates the module is enabled; ✗ indicates it is disabled.

Training-time TTReg: GTM and CFR. Table 6 toggles the two components inside TTReg while keeping the rest of DEViL unchanged. The baseline without TTReg reaches 53.3/35.5 m_tIoU/m_vIoU on HC-STVG v1 and 57.4/35.8 on v2. Enabling **GTM** alone, which selects tubes using the temporal cost C_{temp} in Eq. (4), yields consistent improvements in both datasets. Activating **CFR** alone, which applies the feature and geometric consistency losses $\mathcal{L}_{\text{feat}}$ and $\mathcal{L}_{\text{geom}}$ in Eq. (5), further increases m_tIoU. Combining **GTM+CFR** gives the best overall trade-off, achieving 54.7/36.2 on v1 and 58.0/36.5 on v2. These trends confirm that GTM mines cleaner ground-truth-aligned tubes, while CFR stabilizes query features and boxes across frames; together they yield the most temporally and spatially consistent object tubes.

Test-time MTA with/without TTReg. Table 7 studies the effect of Memory-based Tube Association (MTA) in Eq. (3) under models trained with or without TTReg. Without TTReg, turning on MTA improves m_vIoU from 34.9 to 35.5 on v1 and from 35.4 to 35.8 on v2, while m_tIoU remains unchanged, showing that purely re-associating

TTReg (train)	MTA (test)	HC-STVG v1		HC-STVG v2	
		m_tIoU	m_vIoU	m_tIoU	m_vIoU
✗	✗	53.3	34.9	57.4	35.4
✗	✓	53.3	35.5	57.4	35.8
✓	✗	54.7	35.8	58.0	35.9
✓	✓	54.7	36.2	58.0	36.5

Table 7. Effect of Memory-based Tube Association (MTA) at test time on HC-STVG v1/v2. We compare models trained with or without TTReg and toggle MTA in the OVD decoder. MTA consistently improves m_vIoU while keeping m_tIoU unchanged, and yields the largest gains when combined with TTReg.

queries across frames already refines spatial coverage. When the model is trained with full TTReg (GTM+CFR), enabling MTA further boosts m_vIoU from 35.8 to 36.2 on v1 and from 35.9 to 36.5 on v2, again without affecting m_tIoU. This confirms that MTA is a lightweight test-time plug-in that enhances the tracking behavior of the OVD, and that its benefits are amplified when the detector has been temporally regularized by TTReg.

5. Conclusion

In this paper, we present **DEViL**, a detector-empowered video MLLM for joint temporal and spatial grounding in fine-grained multimodal understanding. Architecturally, we introduce a *Reference–Semantic Token* (RST) that replaces the detector’s text embedding, injecting language-side query semantics into an open-vocabulary detector for geometry-aware localization. We further propose *Tube-Mined Temporal Regularization* (TTReg), which mines a GT-aligned tube and applies cross-frame constraints to stabilize association and reduce drift. To facilitate learning, we adopt a progressive curriculum that sequentially builds bridging, temporal alignment, and spatio-temporal collabora-

ration. Experiments show that DEViL achieves strong results across STVG, TVG, GVQA, and general video benchmarks. Ablations confirm the effectiveness of RST, TTReg, and a lightweight test-time memory association, highlighting the benefit of coupling MLLMs with detectors for robust fine-grained grounding.

References

- [1] Lisa Anne Hendricks, Oliver Wang, Eli Shechtman, Josef Sivic, Trevor Darrell, and Bryan Russell. Localizing moments in video with natural language. In *IEEE/CVF International Conference on Computer Vision (ICCV)*, pages 5803–5812, 2017. [2](#)
- [2] Stanislaw Antol, Aishwarya Agrawal, Jiasen Lu, Margaret Mitchell, Dhruv Batra, C. Lawrence Zitnick, and Devi Parikh. Vqa: Visual question answering. In *IEEE International Conference on Computer Vision (ICCV)*, 2015. [1](#)
- [3] Shuai Bai, Kefin Chen, Xuejing Liu, Jialin Wang, Wenbin Ge, Sibo Song, Kai Dang, Peng Wang, Shijie Wang, Jun Tang, et al. Qwen2. 5-vl technical report. *arXiv preprint arXiv:2502.13923*, 2025. [5](#)
- [4] Zechen Bai, Tong He, Haiyang Mei, Pichao Wang, Ziteng Gao, Joya Chen, Zheng Zhang, and Mike Zheng Shou. One token to seg them all: Language instructed reasoning segmentation in videos. *Advances in Neural Information Processing Systems (NeurIPS)*, 37:6833–6859, 2024. [2](#)
- [5] Nicolas Carion, Francisco Massa, Gabriel Synnaeve, Nicolas Usunier, Alexander Kirillov, and Sergey Zagoruyko. End-to-end object detection with transformers. In *European conference on computer vision (ECCV)*, 2020. [6](#)
- [6] David L. Chen and William B. Dolan. Collecting highly parallel data for paraphrase evaluation. In *Annual Meeting of the Association for Computational Linguistics (ACL)*, 2011. [1](#)
- [7] Shimin Chen, Xiaohan Lan, Yitian Yuan, Zequn Jie, and Lin Ma. Timemarker: A versatile video-llm for long and short video understanding with superior temporal localization ability. *arXiv preprint arXiv:2411.18211*, 2024. [7](#)
- [8] Xin Chen, Ben Kang, Wanting Geng, Jiawen Zhu, Yi Liu, Dong Wang, and Huchuan Lu. Sutrack: Towards simple and unified single object tracking. In *AAAI Conference on Artificial Intelligence (AAAI)*, 2025. [5, 3](#)
- [9] Zhe Chen, Weiyun Wang, Yue Cao, Yangzhou Liu, Zhangwei Gao, Erfei Cui, Jinguo Zhu, Shenglong Ye, Hao Tian, Zhaoyang Liu, et al. Expanding performance boundaries of open-source multimodal models with model, data, and test-time scaling. *arXiv preprint arXiv:2412.05271*, 2024. [5](#)
- [10] Zesen Cheng, Sicong Leng, Hang Zhang, Yifei Xin, Xin Li, Guanzheng Chen, Yongxin Zhu, Wenqi Zhang, Ziyang Luo, Deli Zhao, et al. Videollama 2: Advancing spatial-temporal modeling and audio understanding in video-llms. *arXiv preprint arXiv:2406.07476*, 2024. [7](#)
- [11] Zixu Cheng, Jian Hu, Ziquan Liu, Chenyang Si, Wei Li, and Shaogang Gong. V-star: Benchmarking video-llms on video spatio-temporal reasoning. *arXiv preprint arXiv:2503.11495*, 2025. [5, 6](#)
- [12] Gheorghe Comanici, Eric Bieber, Mike Schaeckermann, Ice Pasupat, Noveen Sachdeva, Inderjit Dhillon, Marcel Blissestein, Ori Ram, Dan Zhang, Evan Rosen, et al. Gemini 2.5: Pushing the frontier with advanced reasoning, multimodality, long context, and next generation agentic capabilities. *arXiv preprint arXiv:2507.06261*, 2025. [5](#)
- [13] Chaoyou Fu, Yuhuan Dai, Yongdong Luo, Lei Li, Shuhuai Ren, Renrui Zhang, Zihan Wang, Chenyu Zhou, Yunhang Shen, Mengdan Zhang, et al. Video-mme: The first-ever comprehensive evaluation benchmark of multi-modal llms in video analysis. In *IEEE/CVF Conference on Computer Vision and Pattern Recognition (CVPR)*, 2025. [7](#)
- [14] Tsu-Jui Fu, Linjie Li, Zhe Gan, Kevin Lin, William Yang Wang, Lijuan Wang, and Zicheng Liu. Violet: End-to-end video-language transformers with masked visual-token modeling. *arXiv preprint arXiv:2111.12681*, 2021. [7](#)
- [15] Jiyang Gao, Chen Sun, Zhenheng Yang, and Ram Nevatia. Tall: Temporal activity localization via language query. In *IEEE/CVF International Conference on Computer Vision (ICCV)*, pages 5267–5275, 2017. [7](#)
- [16] Yash Goyal, Tejas Khot, Douglas Summers-Stay, Dhruv Batra, and Devi Parikh. Making the v in vqa matter: Elevating the role of image understanding in visual question answering. In *IEEE Conference on Computer Vision and Pattern Recognition (CVPR)*, 2017. [1](#)
- [17] Kristen Grauman, Andrew Westbury, Eugene Byrne, Zachary Chavis, Antonino Furnari, Rohit Girdhar, Jackson Hamburger, Hao Jiang, Miao Liu, Xingyu Liu, et al. Ego4d: Around the world in 3,000 hours of egocentric video. In *IEEE/CVF Conference on Computer Vision and Pattern Recognition (CVPR)*, pages 18995–19012, 2022. [2](#)
- [18] Madeleine Grunde-McLaughlin, Ranjay Krishna, and Maneesh Agrawala. Agqa: A benchmark for compositional spatio-temporal reasoning. In *IEEE/CVF Conference on Computer Vision and Pattern Recognition (CVPR)*, 2021. [2](#)
- [19] Xin Gu, Heng Fan, Yan Huang, Tiejian Luo, and Libo Zhang. Context-guided spatio-temporal video grounding. In *IEEE/CVF Conference on Computer Vision and Pattern Recognition (CVPR)*, 2024. [6, 7](#)
- [20] Xin Gu, Yaojie Shen, Chenxi Luo, Tiejian Luo, Yan Huang, Yuewei Lin, Heng Fan, and Libo Zhang. Knowing your target: Target-aware transformer makes better spatio-temporal video grounding. *arXiv preprint arXiv:2502.11168*, 2025. [6, 7](#)
- [21] Yongxin Guo, Jingyu Liu, Mingda Li, Qingbin Liu, Xi Chen, and Xiaoying Tang. Trace: Temporal grounding video llm via causal event modeling. *arXiv preprint arXiv:2410.05643*, 2024. [2, 5](#)
- [22] Yongxin Guo, Jingyu Liu, Mingda Li, Dingxin Cheng, Xiaoying Tang, Dianbo Sui, Qingbin Liu, Xi Chen, and Kevin Zhao. Vtg-llm: Integrating timestamp knowledge into video llms for enhanced video temporal grounding. In *AAAI Conference on Artificial Intelligence (AAAI)*, 2025. [2, 7](#)
- [23] Michael Gygli, Helmut Grabner, Hayko Riemenschneider, and Luc Van Gool. Creating summaries from user videos. In *European Conference on Computer Vision (ECCV)*, 2014. [1](#)
- [24] Edward J Hu, Yelong Shen, Phillip Wallis, Zeyuan Allen-Zhu, Yuanzhi Li, Shean Wang, Lu Wang, Weizhu Chen, et al.

Lora: Low-rank adaptation of large language models. *International Conference on Learning Representations (ICLR)*, 1(2):3, 2022. 4, 6

[25] Bin Huang, Xin Wang, Hong Chen, Zihan Song, and Wenwu Zhu. Vtimellm: Empower llm to grasp video moments. In *IEEE/CVF Conference on Computer Vision and Pattern Recognition (CVPR)*, pages 14271–14280, 2024. 2, 5, 7

[26] De-An Huang, Shijia Liao, Subhashree Radhakrishnan, Hongxu Yin, Pavlo Molchanov, Zhiding Yu, and Jan Kautz. Lita: Language instructed temporal-localization assistant. In *European conference on computer vision (ECCV)*, pages 202–218. Springer, 2024. 2

[27] Aaron Hurst, Adam Lerer, Adam P Goucher, Adam Perelman, Aditya Ramesh, Aidan Clark, AJ Ostrow, Akila Welihinda, Alan Hayes, Alec Radford, et al. Gpt-4o system card. *arXiv preprint arXiv:2410.21276*, 2024. 5

[28] Yang Jin, Zehuan Yuan, Yadong Mu, et al. Embracing consistency: A one-stage approach for spatio-temporal video grounding. *Advances in Neural Information Processing Systems (NeurIPS)*, 35, 2022. 6, 7

[29] Kumara Kahatapitiya, Kanchana Ranasinghe, Jongwoo Park, and Michael S Ryoo. Language repository for long video understanding. In *Findings of the Association for Computational Linguistics: ACL*, pages 5627–5646, 2025. 7

[30] Sahar Kazemzadeh, Vicente Ordonez, Mark Matten, and Tamara Berg. Referitgame: Referring to objects in photographs of natural scenes. In *Proceedings of the 2014 conference on empirical methods in natural language processing (EMNLP)*, pages 787–798, 2014. 5

[31] Ranjay Krishna, Kenji Hata, Frederic Ren, Li Fei-Fei, and Juan Carlos Niebles. Dense-captioning events in videos. In *IEEE/CVF International Conference on Computer Vision (ICCV)*, pages 706–715, 2017. 5, 3

[32] Jie Lei, Licheng Yu, Tamara L. Berg, and Mohit Bansal. TVQQA+: Spatio-temporal grounding for video question answering. In *Annual Meeting of the Association for Computational Linguistics (ACL)*, 2020. 1

[33] Jie Lei, Tamara L Berg, and Mohit Bansal. Detecting moments and highlights in videos via natural language queries. *Advances in Neural Information Processing Systems (NeurIPS)*, 34:11846–11858, 2021. 5, 3

[34] Feng Li, Rennui Zhang, Hao Zhang, Yuanhan Zhang, Bo Li, Wei Li, Zejun Ma, and Chunyuan Li. Llava-next-interleave: Tackling multi-image, video, and 3d in large multimodal models. *arXiv preprint arXiv:2407.07895*, 2024. 7

[35] Hongyu Li, Jinyu Chen, Ziyu Wei, Shaofei Huang, Tianrui Hui, Jialin Gao, Xiaoming Wei, and Si Liu. Llava-ST: A multimodal large language model for fine-grained spatial-temporal understanding. In *IEEE/CVF Conference on Computer Vision and Pattern Recognition (CVPR)*, pages 8592–8603, 2025. 5, 7

[36] Hongyu Li, Jinyu Chen, Ziyu Wei, Shaofei Huang, Tianrui Hui, Jialin Gao, Xiaoming Wei, and Si Liu. Llava-st: A multimodal large language model for fine-grained spatial-temporal understanding. In *IEEE/CVF Conference on Computer Vision and Pattern Recognition (CVPR)*, 2025. 1, 2, 5, 6, 7, 3, 4

[37] KunChang Li, Yinan He, Yi Wang, Yizhuo Li, Wenhui Wang, Ping Luo, Yali Wang, Limin Wang, and Yu Qiao. Videochat: Chat-centric video understanding. *arXiv preprint arXiv:2305.06355*, 2023. 2, 7

[38] Kunchang Li, Yali Wang, Yinan He, Yizhuo Li, Yi Wang, Yi Liu, Zun Wang, Jilan Xu, Guo Chen, Ping Luo, et al. Mvbench: A comprehensive multi-modal video understanding benchmark. In *IEEE/CVF Conference on Computer Vision and Pattern Recognition (CVPR)*, pages 22195–22206, 2024. 5, 7

[39] Tianming Liang, Kun-Yu Lin, Chaolei Tan, Jianguo Zhang, Wei-Shi Zheng, and Jian-Fang Hu. Referdino: Referring video object segmentation with visual grounding foundations. In *IEEE/CVF International Conference on Computer Vision (ICCV)*, 2025. 3, 4

[40] Bin Lin, Yang Ye, Bin Zhu, Jiaxi Cui, Munan Ning, Peng Jin, and Li Yuan. Video-llava: Learning united visual representation by alignment before projection. In *Proceedings of the 2024 Conference on Empirical Methods in Natural Language Processing (EMNLP)*, pages 5971–5984, 2024. 7

[41] Lang Lin, Xueyang Yu, Ziqi Pang, and Yu-Xiong Wang. Glus: Global-local reasoning unified into a single large language model for video segmentation. In *IEEE/CVF Conference on Computer Vision and Pattern Recognition (CVPR)*, pages 8658–8667, 2025. 2

[42] Zihang Lin, Chaolei Tan, Jian-Fang Hu, Zhi Jin, Tiancai Ye, and Wei-Shi Zheng. Collaborative static and dynamic vision-language streams for spatio-temporal video grounding. In *IEEE/CVF Conference on Computer Vision and Pattern Recognition (CVPR)*, 2023. 6, 7

[43] Shilong Liu, Zhaoyang Zeng, Tianhe Ren, Feng Li, Hao Zhang, Jie Yang, Qing Jiang, Chunyuan Li, Jianwei Yang, Hang Su, et al. Grounding DINO: Marrying dino with grounded pre-training for open-set object detection. In *European Conference on Computer Vision (ECCV)*. Springer, 2024. 4, 6

[44] Yuanxin Liu, Shicheng Li, Yi Liu, Yuxiang Wang, Shuhuai Ren, Lei Li, Sishuo Chen, Xu Sun, and Lu Hou. Tempcompass: Do video llms really understand videos? *arXiv preprint arXiv:2403.00476*, 2024. 7

[45] Ze Liu, Yutong Lin, Yue Cao, Han Hu, Yixuan Wei, Zheng Zhang, Stephen Lin, and Baining Guo. Swin transformer: Hierarchical vision transformer using shifted windows. In *IEEE/CVF Conference on Computer Vision and Pattern Recognition (CVPR)*, 2021. 6

[46] Zuyan Liu, Yuhao Dong, Ziwei Liu, Winston Hu, Jiwen Lu, and Yongming Rao. Oryx mllm: On-demand spatial-temporal understanding at arbitrary resolution. *arXiv preprint arXiv:2409.12961*, 2024. 5

[47] Ruiyu Luo, Ziwang Zhao, Min Yang, Junwei Dong, Da Li, Pengcheng Lu, Tao Wang, Linmei Hu, Minghui Qiu, and Zhongyu Wei. Valley: Video assistant with large language model enhanced ability. *arXiv preprint arXiv:2306.07207*, 2023. 7

[48] Muhammad Maaz, Hanoona Rasheed, Salman Khan, and Fahad Khan. Video-chatgpt: Towards detailed video understanding via large vision and language models. In *Proceedings of the 62nd Annual Meeting of the Association for*

Computational Linguistics (Volume 1: Long Papers), pages 12585–12602, 2024. 2, 7

[49] Junhua Mao, Jonathan Huang, Alexander Toshev, Oana Camburu, Alan L Yuille, and Kevin Murphy. Generation and comprehension of unambiguous object descriptions. In *IEEE/CVF Conference on Computer Vision and Pattern Recognition (CVPR)*, pages 11–20, 2016. 5

[50] Jiahao Meng, Xiangtai Li, Haochen Wang, Yue Tan, Tao Zhang, Lingdong Kong, Yunhai Tong, Anran Wang, Zhiyang Teng, Yujing Wang, et al. Open-o3 video: Grounded video reasoning with explicit spatio-temporal evidence. *arXiv preprint arXiv:2510.20579*, 2025. 2

[51] Long Qian, Juncheng Li, Yu Wu, Yaobo Ye, Hao Fei, Tat-Seng Chua, Yuetong Zhuang, and Siliang Tang. Momen-tor: Advancing video large language model with fine-grained temporal reasoning. *arXiv preprint arXiv:2402.11435*, 2024. 2, 7

[52] Rui Qian, Xiaoyi Dong, Pan Zhang, Yuhang Zang, Shuangrui Ding, Dahua Lin, and Jiaqi Wang. Streaming long video understanding with large language models. *Advances in Neural Information Processing Systems (NeurIPS)*, 37:119336–119360, 2024. 7

[53] Nikhila Ravi, Valentin Gabeur, Yuan-Ting Hu, Ronghang Hu, Chaitanya Ryali, Tengyu Ma, Haitham Khedr, Roman Rädle, Chloe Rolland, Laura Gustafson, et al. Sam 2: Segment anything in images and videos. *arXiv preprint arXiv:2408.00714*, 2024. 5, 3

[54] Michaela Regneri, Marcus Rohrbach, Dominikus Wetzel, Stefan Thater, Bernt Schiele, and Manfred Pinkal. Grounding action descriptions in videos. *Transactions of the Association for Computational Linguistics (TACL)*, 1:25–36, 2013. 5, 3

[55] Shuhuai Ren, Linli Yao, Shicheng Li, Xu Sun, and Lu Hou. Timechat: A time-sensitive multimodal large language model for long video understanding. In *IEEE/CVF Conference on Computer Vision and Pattern Recognition (CVPR)*, pages 14313–14323, 2024. 2, 5, 7

[56] Haozhan Shen, Peng Liu, Jingcheng Li, Chunxin Fang, Yibo Ma, Jiajia Liao, Qiaoli Shen, Zilun Zhang, Kangjia Zhao, Qianqian Zhang, et al. Vlm-r1: A stable and generalizable r1-style large vision-language model. *arXiv preprint arXiv:2504.07615*, 2025. 5, 3

[57] Enxin Song, Wenhao Chai, Guanhong Wang, Yucheng Zhang, Haoyang Zhou, Feiyang Wu, Haozhe Chi, Xun Guo, Tian Ye, Yanting Zhang, et al. Moviechat: From dense token to sparse memory for long video understanding. In *IEEE/CVF Conference on Computer Vision and Pattern Recognition (CVPR)*, 2024. 2

[58] Yale Song, Jordi Vallmitjana, Amanda Stent, and Alejandro Jaimes. Tvsun: Summarizing web videos using titles. In *IEEE Conference on Computer Vision and Pattern Recognition (CVPR)*, 2015. 1

[59] Rui Su, Qian Yu, and Dong Xu. STVGBERT: A visual-linguistic transformer based framework for spatio-temporal video grounding. In *IEEE/CVF Conference on Computer Vision and Pattern Recognition (CVPR)*, 2021. 6

[60] Zongheng Tang, Yue Liao, Si Liu, Guanbin Li, Xiaojie Jin, Hongxu Jiang, Qian Yu, and Dong Xu. Human-centric spatio-temporal video grounding with visual transformers. *IEEE Transactions on Circuits and Systems for Video Technology (TCSVT)*, 32(12):8238–8249, 2021. 5, 6, 7, 2, 3, 4

[61] Haibo Wang, Zhiyang Xu, Yu Cheng, Shizhe Diao, Yufan Zhou, Yixin Cao, Qifan Wang, Weifeng Ge, and Lifu Huang. Grounded-videollm: Sharpening fine-grained temporal grounding in video large language models. *arXiv preprint arXiv:2410.03290*, 2024. 2, 7

[62] Jiankang Wang, Zhihan Zhang, Zhihang Liu, Yang Li, Jian-nan Ge, Hongtao Xie, and Yongdong Zhang. Spacevllm: Endowing multimodal large language model with spatio-temporal video grounding capability. *arXiv preprint arXiv:2503.13983*, 2025. 2

[63] Yueqian Wang, Xiaojun Meng, Jianxin Liang, Yuxuan Wang, Qun Liu, and Dongyan Zhao. Hawkeye: Training video-text llms for grounding text in videos. *arXiv preprint arXiv:2403.10228*, 2024. 2, 7

[64] Junbin Xiao, Angela Yao, Yicong Li, and Tat-Seng Chua. Can i trust your answer? video question answering. In *IEEE/CVF Conference on Computer Vision and Pattern Recognition (CVPR)*, 2024. 1, 7

[65] Jun Xu, Tao Mei, Ting Yao, and Yong Rui. Msr-vtt: A large video description dataset for bridging video and language. In *IEEE Conference on Computer Vision and Pattern Recognition (CVPR)*, 2016. 1

[66] Cilin Yan, Haochen Wang, Shilin Yan, Xiaolong Jiang, Yao Hu, Guoliang Kang, Weidi Xie, and Efstratios Gavves. Visa: Reasoning video object segmentation via large language models. In *European conference on computer vision (ECCV)*, pages 98–115. Springer, 2024. 2

[67] Ziang Yan, Zhilin Li, Yinan He, Chenting Wang, Kunchang Li, Xinhao Li, Xiangyu Zeng, Zilei Wang, Yali Wang, Yu Qiao, et al. Task preference optimization: Improving multimodal large language models with vision task alignment. In *IEEE/CVF Conference on Computer Vision and Pattern Recognition (CVPR)*, 2025. 7

[68] Antoine Yang, Antoine Miech, Josef Sivic, Ivan Laptev, and Cordelia Schmid. Tubedetr: Spatio-temporal video grounding with transformers. In *IEEE/CVF Conference on Computer Vision and Pattern Recognition (CVPR)*, 2022. 6, 7

[69] Antoine Yang, Antoine Miech, Josef Sivic, Ivan Laptev, and Cordelia Schmid. Zero-shot video question answering via frozen bidirectional language models. *Advances in Neural Information Processing Systems (NeurIPS)*, 2022. 7

[70] An Yang, Anfeng Li, Baosong Yang, Beichen Zhang, Binyuan Hui, Bo Zheng, Bowen Yu, Chang Gao, Chengan Huang, Chenxu Lv, et al. Qwen3 technical report. *arXiv preprint arXiv:2505.09388*, 2025. 6

[71] Kexin Yi, Chuang Gan, Yunzhu Li, Pushmeet Kohli, Jiajun Wu, Antonio Torralba, and Joshua B. Tenenbaum. Clevrer: Collision events for video representation and reasoning. In *International Conference on Learning Representations (ICLR)*, 2020. 1

[72] Shoubin Yu, Jaemin Cho, Prateek Yadav, and Mohit Bansal. Self-chained image-language model for video localization and question answering. In *Advances in Neural Information Processing Systems (NeurIPS)*, 2023. 7

[73] Haobo Yuan, Xiangtai Li, Tao Zhang, Zilong Huang, Shilin Xu, Shunping Ji, Yunhai Tong, Lu Qi, Jiashi Feng, and Ming-Hsuan Yang. Sa2va: Marrying sam2 with llava for dense grounded understanding of images and videos. *arXiv preprint arXiv:2501.04001*, 2025. 2, 5, 3

[74] Xiaohua Zhai, Basil Mustafa, Alexander Kolesnikov, and Lucas Beyer. Sigmoid loss for language image pre-training. In *IEEE/CVF International Conference on Computer Vision (ICCV)*, 2023. 6

[75] Boqiang Zhang, Kehan Li, Zesen Cheng, Zhiqiang Hu, Yuqian Yuan, Guanzheng Chen, Sicong Leng, Yuming Jiang, Hang Zhang, Xin Li, et al. Videollama 3: Frontier multi-modal foundation models for image and video understanding. *arXiv preprint arXiv:2501.13106*, 2025. 5, 6

[76] Ce Zhang, Taixi Lu, Md Mohaiminul Islam, Ziyang Wang, Shoubin Yu, Mohit Bansal, and Gedas Bertasius. A simple ilm framework for long-range video question-answering. In *Conference on Empirical Methods in Natural Language Processing (EMNLP)*, pages 21715–21737, 2024. 7

[77] Hang Zhang, Xin Li, and Lidong Bing. Video-llama: An instruction-tuned audio-visual language model for video understanding. *arXiv preprint arXiv:2306.02858*, 2023. 2, 7

[78] Yuanhan Zhang, Jinming Wu, Wei Li, Bo Li, Zejun Ma, Ziwei Liu, and Chunyuan Li. Video instruction tuning with synthetic data. *arXiv preprint arXiv:2410.02713*, 2024. 5

[79] Zhu Zhang, Zhou Zhao, Yang Zhao, Qi Wang, Huasheng Liu, and Lianli Gao. Where does it exist: Spatio-temporal video grounding for multi-form sentences. In *IEEE/CVF Conference on Computer Vision and Pattern Recognition (CVPR)*, 2020. 1, 5, 6, 2, 3, 4

[80] Xiangyu Zhao, Yicheng Chen, Shilin Xu, Xiangtai Li, Xinqiang Wang, Yining Li, and Haian Huang. An open and comprehensive pipeline for unified object grounding and detection. *arXiv preprint arXiv:2401.02361*, 2024. 5, 3

1 + 1 > 2: Detector-Empowered Video Large Language Model for Spatio-Temporal Grounding and Reasoning

Supplementary Material

Dataset	#Videos	#Queries	#Samples
HC-STVG v1 [60]	4,500	4,500	4.5k
HC-STVG v2 [60]	10,131	10,131	10k
VidSTG [79]	5,436	80,684	81k
Self-collected (ours)	42,792	101,080	101k

Table 8. **Comparison of HC-STVG v1/v2 [60], VidSTG [79] and our self-collected data** in the Stage-3 spatio-temporal training corpus. Samples is the number of tube-level instances after reformulation and pseudo labels.

Overview

In this appendix, we provide additional descriptions of the following contents:

- Explanation of the exposure bias of textualized box decoding (Sec. 6).
- Detail about Spatio-temporal Training Data (Sec. 7).
- Additional Ablation Studies (Sec. 8).
- Additional Qualitative Analysis (Sec. 9).
- Limitations and Future Work Discussion (Sec. 10).

6. Exposure bias of textualized box decoding

In this section, we explain that textual spatial decoding of LLMs leads to very long output sequences, causing spatial errors to accumulate over time.

Given textual features \mathbf{Q} and video features \mathbf{V} , LLMs employ a textualized box decoder to predict a sequence of tokens $\mathbf{y}_{1:L} = (y_1, \dots, y_L)$ (covering all frame-wise boxes and timestamps) in an autoregressive way:

$$p(\mathbf{y}_{1:L} | \mathbf{Q}, \mathbf{V}) = \prod_{l=1}^L p(y_l | \mathbf{y}_{<l}, \mathbf{Q}, \mathbf{V}). \quad (7)$$

During training, teacher forcing feeds ground-truth tokens $\mathbf{y}_{<l}^*$ at every step:

$$\mathcal{L}_{\text{train}} = - \sum_{l=1}^L \log p(y_l^* | \mathbf{y}_{<l}^*, \mathbf{Q}, \mathbf{V}), \quad (8)$$

while at inference the model conditions on its own predictions $\hat{\mathbf{y}}_{<l}$:

$$\hat{y}_l \sim p(y_l | \hat{\mathbf{y}}_{<l}, \mathbf{Q}, \mathbf{V}), \quad \hat{\mathbf{y}}_{1:L} = (\hat{y}_1, \dots, \hat{y}_L), \quad (9)$$

which induces a train–test mismatch, *i.e.*, exposure bias.

Assuming that, when the history is clean, each step predicts the correct token with probability $p_s = 1 - \varepsilon$. Ignoring

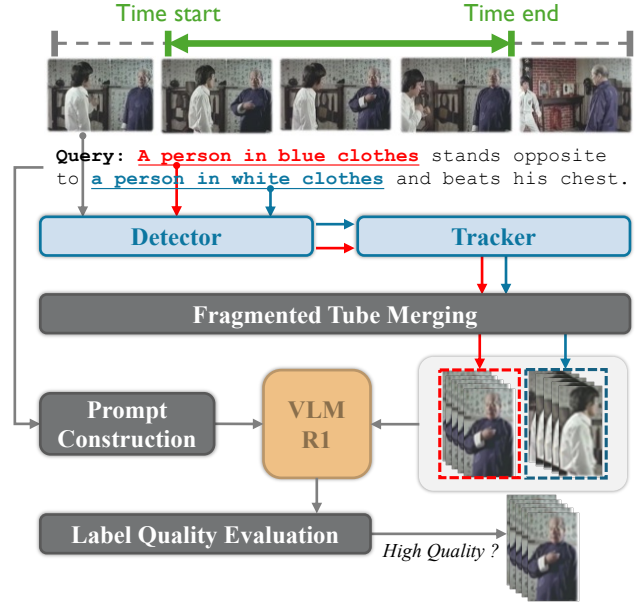


Figure 5. **Auto-labeling process** used to translate temporal video grounding datasets to spatio-temporal video grounding datasets.

higher-order correlations, the probability that the whole textualized box sequence is error-free satisfies

$$P[\hat{\mathbf{y}}_{1:L} = \mathbf{y}_{1:L}^*] = p_s^L = (1 - \varepsilon)^L \approx 1 - L\varepsilon \quad (\varepsilon \ll 1), \quad (10)$$

so the failure probability grows approximately linearly in the sequence length L . For spatio-temporal grounding, each frame-level box is represented by multiple discrete tokens, and long videos further increase L , making the model especially vulnerable: an early coordinate error shifts the decoded box away from the target, then all subsequent steps condition on this misaligned textual history instead of the true visual evidence, causing accumulated errors and visible localization drift over time.

7. Spatio-Temporal Training Data Detail

In the third training stage of DEViL, we mix existing datasets with our self-collected data and automatically label them to train the model’s generalized spatio-temporal grounding capability. Table 8 summarizes the differences between these sources. In the following, We first describe the self-collected data and the auto-labeling pipeline, and then introduce the instruction-style reformulation applied to the existing datasets.

Model	HC-STVG v1				Time	HC-STVG v2				Time
	m.tIoU	m.vIoU	vIoU@0.3	vIoU@0.5		m.tIoU	m.vIoU	vIoU@0.3	vIoU@0.5	
LLaVA-ST* [36]	22.2	9.4	8.1	2.8	2.22h	21.6	8.7	6.0	1.2	4.02h
DEViL*	47.0	24.8	37.8	17.0	1.92h	52.9	28.0	43.8	21.1	3.50h
DEViL	54.7	36.2	59.9	31.8	1.92h	58.0	36.5	58.0	31.8	3.50h
Model	VidSTG (Declarative)				VidSTG (Interrogative)				Time	
	m.tIoU	m.vIoU	vIoU@0.3	vIoU@0.5	m.tIoU	m.vIoU	vIoU@0.3	vIoU@0.5		
LLaVA-ST [36]	28.7	8.2	10.6	5.0	27.5	6.8	8.3	3.9	43.75h	
DEViL*	44.4	25.2	32.8	22.7	43.2	18.2	22.8	15.1	15.43h	
DEViL	49.0	32.0	43.7	30.7	47.3	27.7	37.5	25.5	15.43h	

Table 9. Spatio-temporal video grounding results on HC-STVG v1 [60], HC-STVG v2 [60] and VidSTG [79]. Rows marked with * are zero-shot settings: LLaVA-ST* is directly evaluated on each dataset without further training on it, while DEViL* is trained only on the self-collected corpus and evaluated zero-shot on all three benchmarks. Time is the total inference time to run each test set once on a single NVIDIA A800 GPU.

Self-collected Data for Training. Our self-collected dataset consists of two main parts: video segmentation datasets and temporal video grounding datasets. First, following Sa2VA [73], we start from Ref-SAV [73] derived from SA-V [53]. For each annotated object, we convert its segmentation masks into tight bounding boxes and align them with the annotated visible time span of the object. This produces tube-level labels consisting of a start/end timestamp and a per-frame bounding box, providing dense spatial supervision for short clips. Second, we lift temporal video grounding (TVG) datasets, *i.e.*, TACoS [54], ActivityNet Captions [31], QVHighlights [33], into spatio-temporal tubes. Considering these datasets only provide temporal segments and text queries as the original annotations, we build an automatic labeling pipeline to supplement the object tubes.

Auto-labeling Pipeline. As illustrated in Fig. 5, our auto-labeling pipeline for TVG datasets combines (i) a strong open-vocabulary detector (MM-GroundingDINO [80]), (ii) a referring-expression VLM (VLM-R1 [56]), and (iii) a visual tracker (SUTrack [8]). Given a text query and its originally-annotated temporal interval, we first apply a detector-tracker pipeline to detect and track all objects mentioned in this query. Next, to alleviate fragmented object tubes, we merge per-segment object tubes that belong to the same category and exhibit similar appearance but occur at different times, forming complete object tubes as candidate results. Then, leveraging VLM-R1 with powerful reasoning capability, we select, from all candidates, the tube that best matches the text query. Finally, since the selected tube may not fully cover the annotated interval, we discard the produced annotation, *i.e.*, the best tube, if this tube overlaps with less than 50% of the frames in the given interval. Otherwise, we retain the selected tube as a pseudo annotation of spatio-temporal video grounding.

Instruction-Style Reformulation. We rewrite the supervision for all stages into concise question–answer instructions.

Stage 1 (Bridge).

Question: "<image> Locate the visual content described by the query <query></query> in the image."
 Answer: "The spatial location of the object is [BOX]."

Stage 2 (Alignment).

Question: "<video> Locate the visual content described by the query <query></query>. Output the start and end timestamps in seconds."
 Answer: "The visual content occurs from t1 to t2."

Stage 3 (Collaboration).

Question: "<video> Locate the visual content described by the query <query></query> in the video. Please output the start and end timestamps in seconds and the spatial location of the object."
 Answer: "The visual content occurs from t1 to t2, and the spatial location of the object is [BOX]."

8. Additional Ablations

We provide three additional ablations to better understand DEViL: zero-shot generalization, frame sampling, and inference efficiency.

Zero-shot STVG from the Self-collected Corpus. Tab. 9 compares different training regimes on HC-STVG v1/v2

T (frames)	HC-STVG v1				HC-STVG v2			
	m.tIoU	m.vIoU	vIoU@0.3	vIoU@0.5	m.tIoU	m.vIoU	vIoU@0.3	vIoU@0.5
32	54.3	35.8	58.2	30.7	57.4	35.8	57.4	31.2
64	54.7	36.2	59.9	31.8	58.0	36.5	58.0	31.8
128	50.3	33.4	53.6	28.7	52.4	32.8	51.5	27.5

Table 10. Effect of the number of sampled frames T at inference on HC-STVG v1 [60] and HC-STVG v2 [60]. We vary T during testing while keeping the training setup fixed and report all four metrics on both datasets.

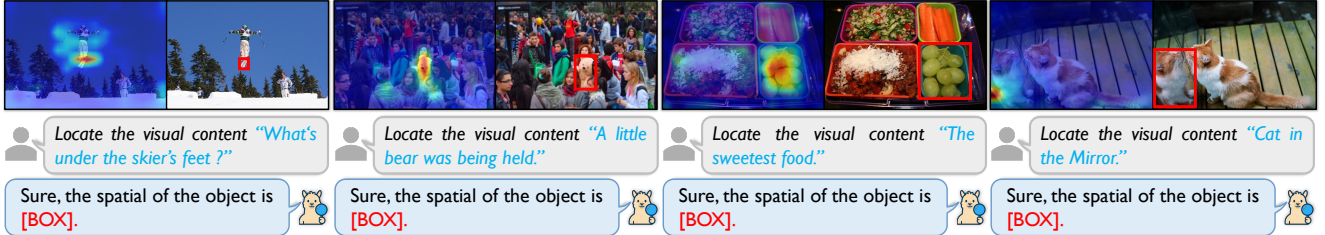


Figure 6. Qualitative examples of image referring expression comprehension: given a natural-language query, our model predicts the spatial location of the target, and the overlaid heatmaps visualize attention between the [BOX]-induced RST/text feature and image features, which concentrates on the queried region.

[60] and VidSTG [79]. Rows marked with * are zero-shot settings. LLaVA-ST* [36] is directly evaluated on each benchmark without further tuning, while DEVIL* is trained only on the self-collected tubes and then evaluated zero-shot. Despite never seeing human-labeled STVG data, DEVIL* outperforms LLaVA-ST* or even LLaVA-ST by large margins on all metrics, and the fully trained DEVIL further improves both temporal and spatial localization.

Effect of the Number of Frames T . Tab. 10 studies the impact of the number of sampled frames T at inference on HC-STVG v1/v2. Keeping the training setup fixed, we find that $T=64$ gives the best trade-off between coverage and noise: using fewer frames ($T=32$) slightly hurts both m.tIoU and m.vIoU due to missing visual evidence, whereas using more frames ($T=128$) introduces redundant or low-quality frames, which makes grounding harder and leads to degraded performance.

Inference Speed Analysis. The time columns in Tab. 9 report the wall-clock time to run each test set once on a single A800 GPU. On HC-STVG v1/v2, DEVIL and LLaVA-ST have similar runtimes because videos are short and the textualized decoder of LLaVA-ST only needs to generate relatively short sequences. On VidSTG, however, videos are much longer and the textualized box decoder must output very long coordinate sequences, so the decoding cost of LLaVA-ST grows quickly and its total runtime reaches 43.75 hours. In contrast, DEVIL keeps the language output short and sends key frames to the OVD in parallel; the detector dominates the cost but scales nearly linearly with the number of frames and is not affected by sequence length.

As a result, DEVIL is about $2.8\times$ faster on VidSTG (15.43 hours) while achieving substantially higher spatio-temporal grounding accuracy.

9. Additional Qualitative Analysis

Figs. 6–11 present additional qualitative results across images and videos. Fig. 6 shows image-level referring expression comprehension, where the predicted [BOX] and its RST-based attention align well with the queried region. Figs. 7 and 8 illustrate spatio-temporal and spatial video grounding with attention consistently focusing on the target object. Fig. 9 highlights temporal event localization, while Fig. 10 shows grounded video QA supported by localized visual evidence. Finally, Fig. 11 demonstrates multi-turn video conversation, where our agent follows free-form instructions and provides explicit spatio-temporal grounding as interpretable evidence.

10. Limitations and Future Work Discussion

Most existing spatio-temporal grounding (STVG) benchmarks adopt a *single-target* setting, where each query corresponds to one dominant object tube. Consequently, DEVIL is trained to emit a single RST and retrieve one tube per query, without explicitly modeling multiple entities or their roles. As future work, we plan to extend DEVIL to *multi-target* grounding by generating multiple entity-specific RSTs and adapting TTReg and the training corpus to maintain temporally consistent tubes in crowded scenes, bringing DEVIL closer to video agents that reason over rich multi-entity interactions.

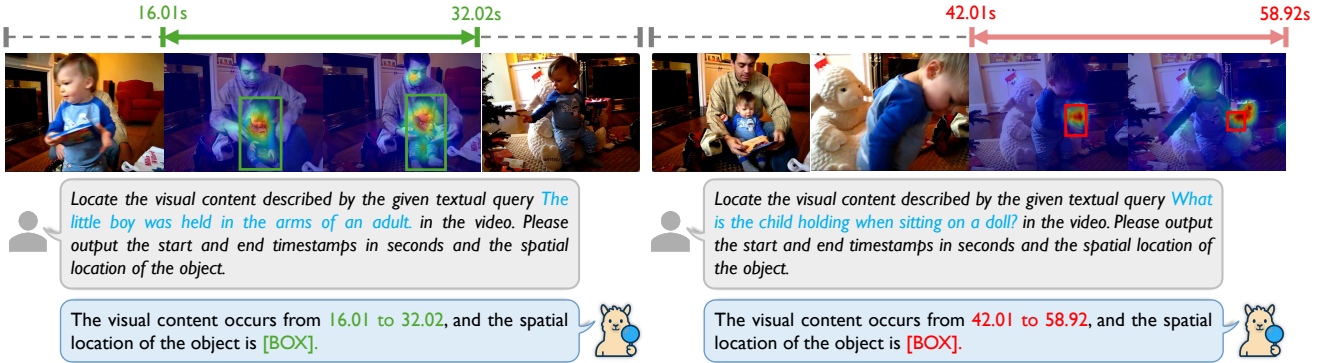


Figure 7. Qualitative examples of spatio-temporal video grounding: given a natural-language query, our model predicts both the time span and the spatial location of the target, and the overlaid heatmaps visualize attention between the [BOX]-induced RST/text feature and video features, concentrating on the described event across time.

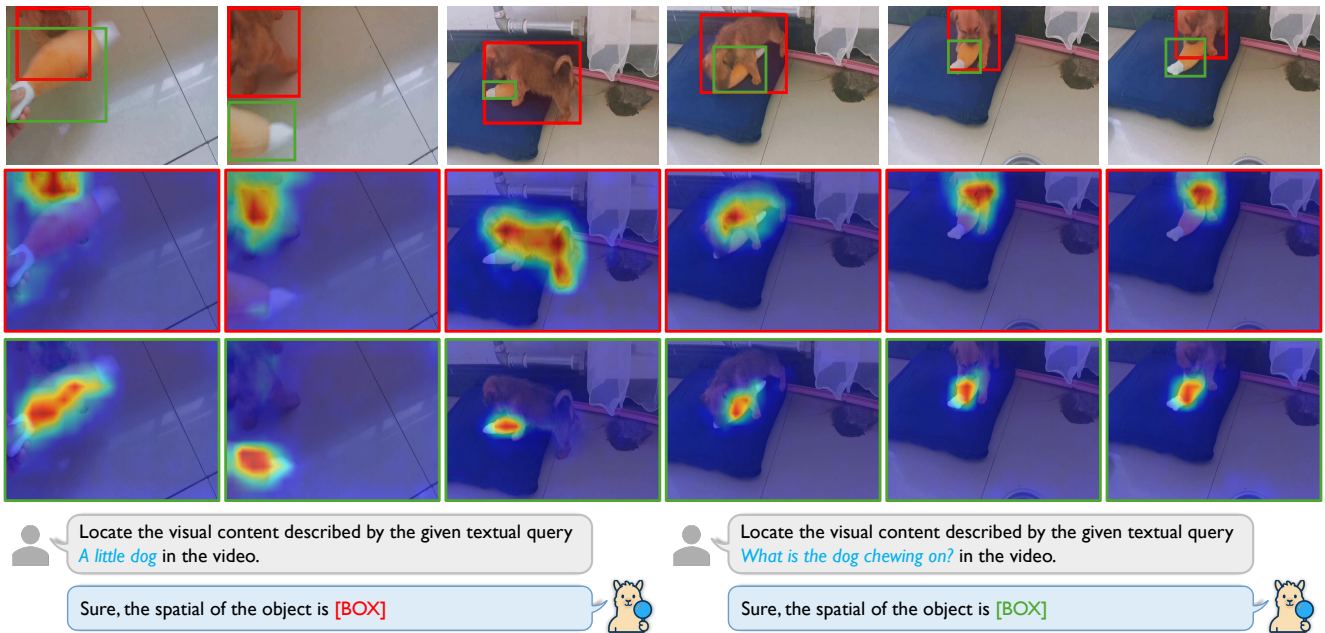


Figure 8. Qualitative examples of spatial video grounding: given a natural-language query, our model predicts the frame-wise spatial location [BOX] of the target, and the overlaid heatmaps visualize attention between the [BOX]-induced RST/text feature and video features, focusing on the queried object across frames.

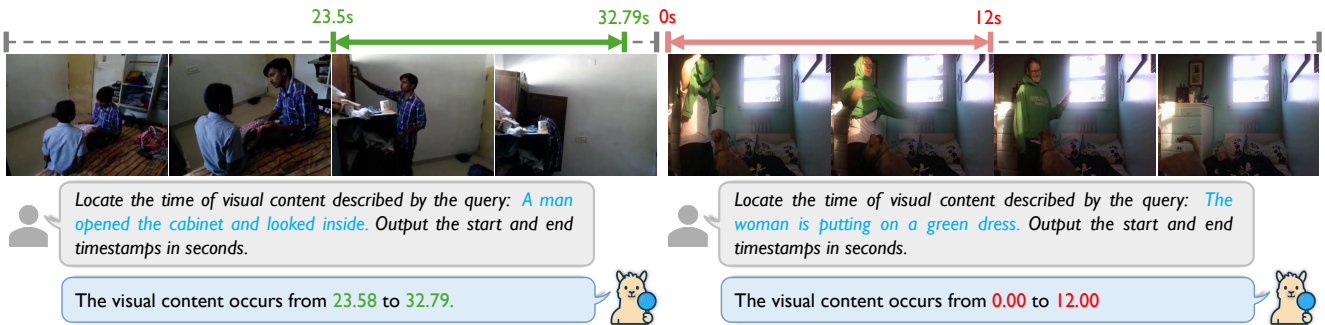


Figure 9. Qualitative examples of temporal video grounding: given a language description, the model returns the start and end times of the corresponding event in the video.

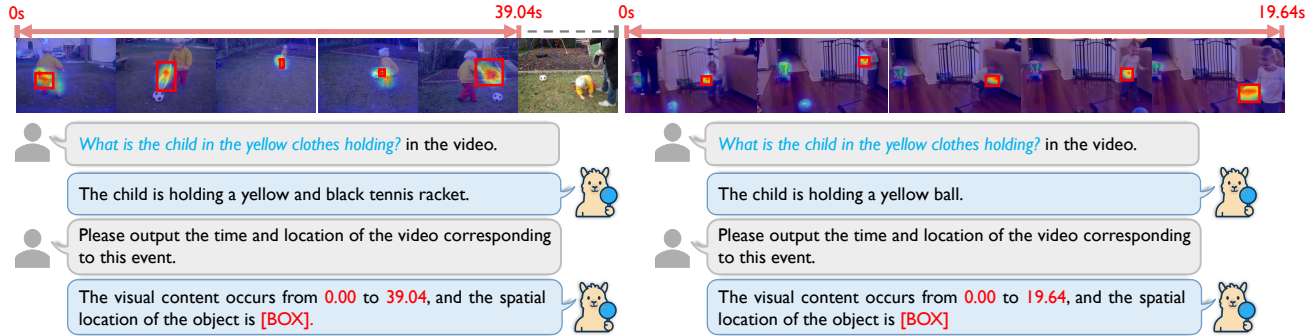


Figure 10. Qualitative examples of grounded video question answering: given a natural-language question, our model first produces an answer and then predicts the time span and spatial location of the corresponding visual evidence, where the overlaid heatmaps visualize attention between the [BOX]-induced RST/text feature and video features, highlighting the evidence along the timeline.

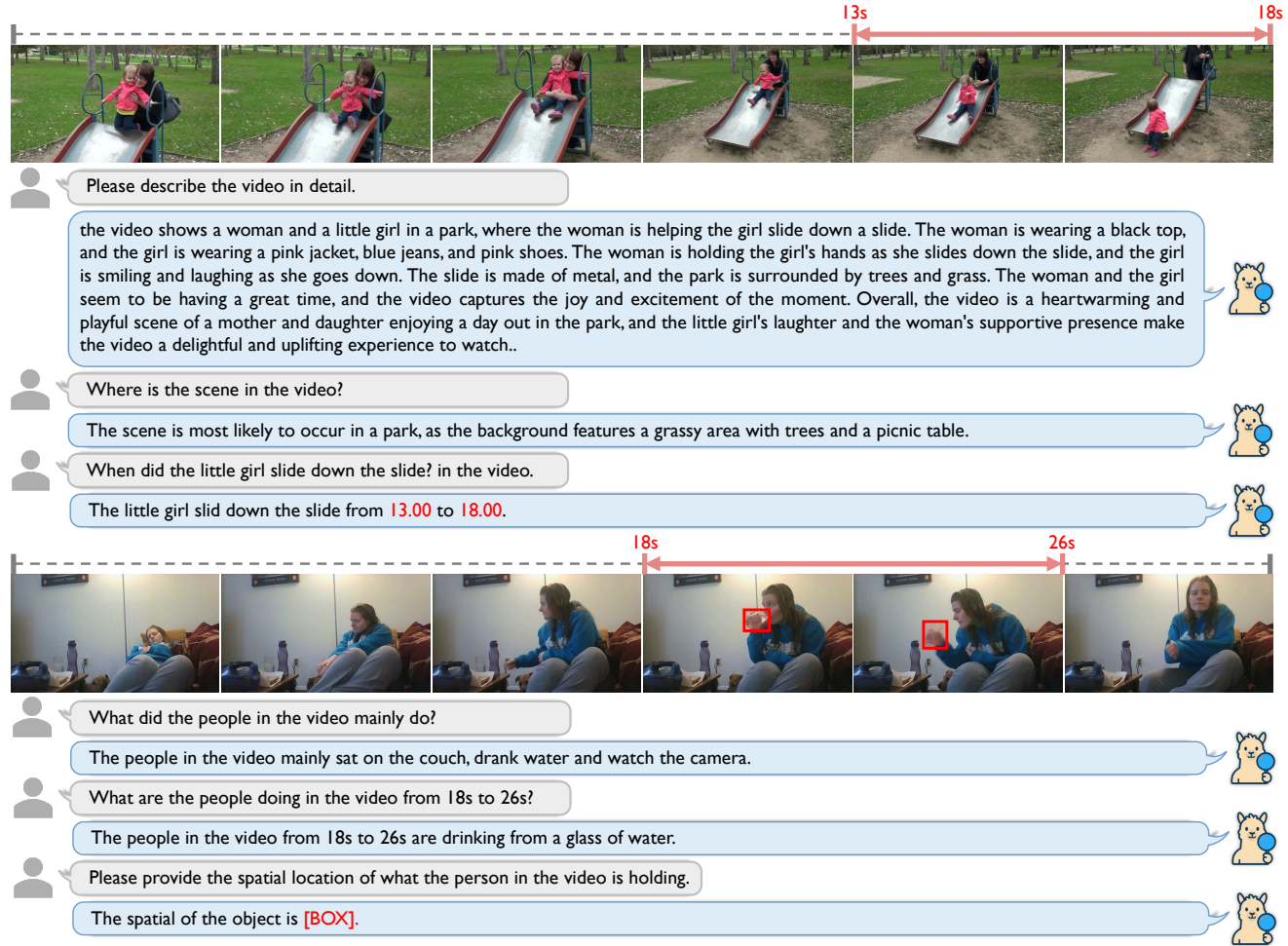


Figure 11. Qualitative examples of multi-turn video conversation: our agent supports free-form descriptions, follow-up questions, and explicit temporal and spatial grounding within the same dialogue.